

Study of Hydrodynamic-Magnetic-Thermal Coupling in a Linear Induction MHD Pump

Fatima Zohra Kadid*, Said Drid** and Rachid Abdessemed*

Abstract – This article deals with the analysis of a coupling between stationary Maxwell's equations, the transient state Navier-Stokes and thermal equations. The resolution of these equations is obtained by introducing the magnetic vector potential \mathbf{A} , the vorticity $\boldsymbol{\xi}$, the stream function ψ and the temperature T . The flux density, the electromagnetic thrust, the electric power density, the velocity, the pressure and the temperature are graphically visualized. Also, the influence of the frequency is presented.

Keywords: Magnetohydrodynamics (MHD), Finite element method (FEM), Finite volume method (FVM), Stream-vorticity formulation, Temperature, Channel, Induction pump

1. Introduction

Magnetohydrodynamics (MHD) and its applications are widespread, and can be found in nuclear reactors, magnetohydrodynamic (MHD) generators, pumps, accelerators and blood flow measurements [1], [2]. MHD is a theory that describes the interaction of an electrically conducting fluid with magnetic fields. Effects from such interactions can be observed in liquids and gases. The pumping of liquid metal may use an electromagnetic device, which induces eddy currents in the metal. These induced currents and their associated magnetic field generate a Lorentz force, the effect of which can be the pumping of liquid metals. The advantage of these pumps which ensure energy transformation is the absence of moving parts. Linear induction MHD pumps are electromagnetic devices that use the principle of induction motors to move liquid metal by the action of a sliding field [3].

The magnetohydrodynamic problem is studied using the finite element method for the electromagnetic problem and the finite volume method for the hydrodynamic and thermal problems.

The difficulty with the electromagnetic problem is the presence of the convective term $\mathbf{V} \wedge \mathbf{B}$ due to the movement of the fluid, where \mathbf{B} is the magnetic induction and \mathbf{V} is the velocity [4-5]. However, in the hydrodynamic study, the problem or difficulty to be solved numerically is due to the incompressibility constraint given by the continuity equation $\text{div} \mathbf{V} = 0$ which couples the velocity \mathbf{V} and the pressure p , and the choice of numerical method. In existing literature Many formulations to solve the problem of incompressibility constraints in Navier-Stokes equations can be found in existing literature.

These include the pseudo-compressibility method, which in turn includes the penalty method [6-7], although this presents a problem with the choice of the penalty coefficient which must be carefully chosen in order to ensure accuracy and convergence; the SIMPLE algorithm [8]; and the stream-vorticity formulation [9], [10]. After simplifications of the Navier-Stokes equations, it is possible to obtain the velocity and the pressure as several methods are used, such as the finite element method [11], the boundary element method [12], and the finite volume method [8]. Consequently, in this paper we chose the stream-vorticity formulation, the most used in hydrodynamics problems in transient cases, and with the use of the finite volume method where the principle of conservation is imposed over each volume of control and therefore easier for comparison to the finite element method [8].

The goal of this paper is to compute the velocity, pressure and temperature of the fluid in the channel of the MHD pump. To do so, it is initially necessary to determine the flux density then the induced currents, the electromagnetic thrust and the thermal source which allow the velocity to be calculated, and the pressure and temperature at any point of the channel. A study of the influence of frequency on fluid flow and temperature is also performed.

2. Electromagnetic Problem

2.1 Mathematical model

Fig. 1 shows the scheme of the MHD pump. It has two inductors which contain the coils, air gap and the external area, while the channel contains the liquid metal. The conducting fluid is assumed to be viscous and incompressible.

For the calculation reported in the following, mercury is considered as the fluid. The equations describing the pumping process in the channel are Maxwell's equations such as:

* Dept. of Electrical and Electronic Engineering, Batna University, Algeria. (fzohra_kadid@hotmail.com)

** Dept. of Electrical and Electronic Engineering, Batna University, Algeria. (s_drid@yahoo.fr)

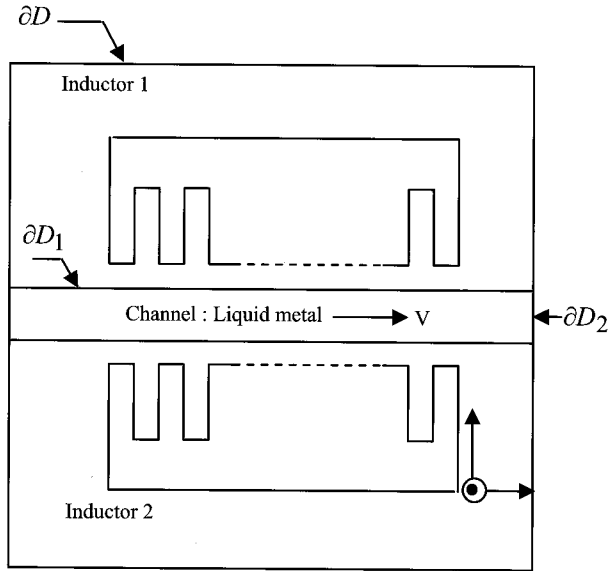


Fig. 1. Schematic view of the MHD pump

$$\text{rot} \left(\frac{1}{\mu} \text{rot} \mathbf{A} \right) + \sigma \left(\frac{\partial \mathbf{A}}{\partial t} - \mathbf{V} \times \text{rot} \mathbf{A} \right) = \mathbf{J}_{\text{ex}} \quad (1)$$

where \mathbf{A} is the magnetic vector potential, σ is the electrical conductivity, μ the magnetic permeability, \mathbf{V} is the velocity of the fluid and \mathbf{J}_{ex} the excitation current density.

After developing the above equations in Cartesian coordinates and in sinusoidal mode, the final integro-differential system with the Dirichlet boundary condition is:

$$-\frac{1}{\mu} \left(\frac{\partial^2 A}{\partial x^2} + \frac{\partial^2 A}{\partial y^2} \right) + \sigma \left(j_w A + V \frac{\partial A}{\partial x} \right) = J_{\text{ex}} \quad (2)$$

$$A = 0 \quad \text{on } \partial D \quad (3)$$

The currents of the windings generate a traveling magnetic field which produces a current in the liquid metal. As a consequence, a Lorentz force acting on the fluid is obtained.

The eddy currents inside the channel are computed by:

$$\mathbf{J}_i = -\sigma \left(\frac{\partial \mathbf{A}}{\partial t} - \mathbf{V} \times \text{rot} \mathbf{A} \right) \quad (4)$$

The thrusts are given by:

$$\mathbf{F} = \mathbf{J}_i \times \text{rot} \mathbf{A} \quad (5)$$

2.2 Finite element method

The system described in (2) and (3) is solved using the finite element method. We apply the weak Galerkin method to the equation (2) which consists to seek n projection functions $\varphi_1, \varphi_2, \dots, \varphi_n$ such as:

$$\int_{\Omega} \varphi_i \left[\frac{1}{\mu} \left(\frac{\partial^2 A}{\partial x^2} + \frac{\partial^2 A}{\partial y^2} \right) \right] d\Omega \quad (6)$$

$$+ \int_{\Omega} \varphi_i \left(-\sigma j_w A + J_{\text{ex}} - \sigma V \frac{\partial A}{\partial x} \right) d\Omega = 0$$

After evaluating the resulting integrals by parts over the whole problem domain (Ω) and then substituting the appropriate boundary conditions, we obtain a set of simultaneous partial differential equations of the form [13], [14]:

$$[j\omega[C] + [M_1] + [M_2]][A] = [F] \quad (7)$$

with:

$$[C] = \int_{\Omega} \sigma \varphi_i \varphi_j d\Omega$$

$$[M_1] = \int_{\Omega} \frac{1}{\mu} \text{grad}(\varphi_i) \text{grad}(\varphi_j) d\Omega$$

$$[M_2] = \int_{\Omega} \sigma V \varphi_i \frac{\partial \varphi_j}{\partial x} d\Omega$$

$$[F] = J_{\text{ex}} \int_{\Omega} \varphi_i d\Omega$$

The matrices $[C]$, $[M_1]$ and $[M_2]$ are calculated considering the element matrices, appropriate shape functions [4], [5] and [14]. The vector $[F]$ accounts for the current J_{ex} . The resulting equations are solved using the iterative method until convergence is reached. Once \mathbf{A} is obtained, we can compute the magnetic induction field by using $\mathbf{B} = \text{rot} \mathbf{A}$.

3. The Hydrodynamic and Thermal Problems

3.1. Navier-Stokes equations

The MHD flows of an incompressible, viscous and electrically conducting fluid in a transient state condition is governed by the Navier-Stokes equations [9]:

$$\frac{\partial \mathbf{V}}{\partial t} + (\nabla \cdot \mathbf{V}) \mathbf{V} = -\frac{1}{\rho} \nabla p + \nu \Delta \mathbf{V} + \frac{\mathbf{F}}{\rho} \quad (8)$$

$$\text{div} \mathbf{V} = 0 \quad (9)$$

where p is the pressure of the fluid, ν the kinematic viscosity of the fluid, \mathbf{F} the electromagnetic thrust and ρ the fluid density.

The development of the equation of the flow in Cartesian coordinates gives:

$$\left\{ \begin{array}{l} \frac{\partial u}{\partial t} + u \frac{\partial u}{\partial x} + u' \frac{\partial u}{\partial y} = -\frac{1}{\rho} \frac{\partial p}{\partial x} + \nu \left(\frac{\partial^2 u}{\partial x^2} + \frac{\partial^2 u}{\partial y^2} \right) + \frac{F_x}{\rho} \\ \frac{\partial u'}{\partial t} + u \frac{\partial u'}{\partial x} + u' \frac{\partial u'}{\partial y} = -\frac{1}{\rho} \frac{\partial p}{\partial y} + \nu \left(\frac{\partial^2 u'}{\partial x^2} + \frac{\partial^2 u'}{\partial y^2} \right) + \frac{F_y}{\rho} \\ \frac{\partial u}{\partial x} + \frac{\partial u'}{\partial y} = 0 \end{array} \right. \quad (10)$$

The boundary conditions are such as:

$$\left\{ \begin{array}{l} u = u' = 0 \quad \text{on } \partial D_1 \\ \frac{\partial u}{\partial n} = 0, \quad \frac{\partial u'}{\partial n} = 0 \quad \text{on } \partial D_2 \end{array} \right. \quad (11)$$

The real difficulty is that the calculation of the velocity

lies in the unknown pressure. To overcome this difficulty is to relax the incompressibility constraint in an appropriate way. Consequently, the elimination of pressure from the equations leads to a vorticity-stream function [9-10]. The vorticity vector is defined by:

$$\xi = \text{rot}V \quad (12)$$

The stream function is given in 2D Cartesian coordinates as:

$$\begin{aligned} \frac{\partial \psi}{\partial y} &= u \\ \frac{\partial \psi}{\partial x} &= -u' \end{aligned} \quad (13)$$

Where u and u' are the components of the velocity V .

We eliminate the pressure from the equation (10) and use the two new dependent variables ξ and Ψ to obtain the following equation:

$$\frac{\partial \xi}{\partial t} + u \frac{\partial \xi}{\partial x} + u' \frac{\partial \xi}{\partial y} = \nu \left(\frac{\partial^2 \xi}{\partial x^2} + \frac{\partial^2 \xi}{\partial y^2} \right) + \frac{1}{\rho} \left(\frac{\partial F_y}{\partial x} - \frac{\partial F_x}{\partial y} \right) \quad (14)$$

After substituting equation (13) into equation (12) we obtain an equation involving the new dependant variables ξ and ψ such as:

$$\frac{\partial^2 \psi}{\partial x^2} + \frac{\partial^2 \psi}{\partial y^2} = -\xi \quad (15)$$

To determine the pressure, the resolution of an additional equation is necessary. The latter is obtained by differentiating equation (8) and using the continuity equation (9). This equation is referred as Poisson's equation for pressure:

$$\Delta p = 2\rho \left(\frac{\partial^2 \psi}{\partial x^2} - \frac{\partial^2 \psi}{\partial y^2} \right) \quad (16)$$

3.2 Thermal problem

The thermal phenomena are studied only in the channel of the MHD pump. As a result, the governing thermal equation is given by:

$$\rho C_p \frac{\partial T}{\partial t} + \frac{T}{\rho} \left(\frac{\partial \rho}{\partial T} \right) \rho \frac{Dp}{Dt} = \text{div}(K \mathbf{grad} T) + p_s \quad (17)$$

where ρ is the density of the fluid, C_p the specific heat, K the thermal conductivity, T the temperature and p_s the thermal source induced by eddy current such as:

$$p_s = \frac{J^2}{2\sigma} \quad (18)$$

After developments in Cartesian coordinates, by replacing the source term p_s and neglecting the term of pressure is due to the low velocities obtained in the hydrodynamic study, we obtain:

$$\rho C_p \frac{\partial T}{\partial t} = K \left[\frac{\partial^2 T}{\partial x^2} + \frac{\partial^2 T}{\partial y^2} \right] + \frac{J_i J_i^*}{2\sigma} \quad (19)$$

J_i^* is the conjugate of J_i .

The thermal boundary conditions are applied to the channel (Fig. 2) as follows:

$$T = 298^\circ\text{K} \text{ on } \partial D_1.$$

$$\text{and } \frac{\partial T}{\partial n} = 0 \text{ on } \partial D_2.$$

4. Numerical Method

For the fluid flow model, there is one control volume surrounding each node (Fig. 2) and the differential equation (14) is integrated over each control volume using the finite volume approach [8]:

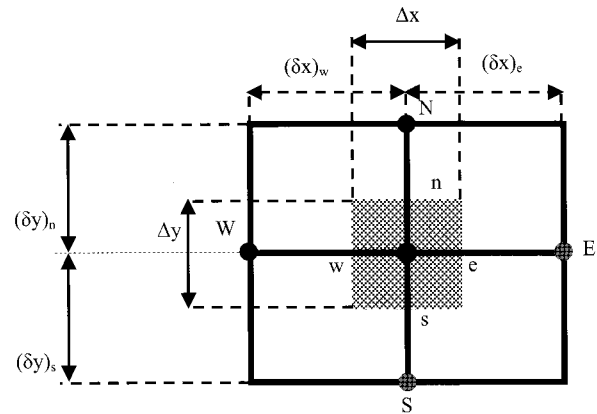


Fig. 2. Discretisation in finite volume method

$$\int_{\Omega} \left(\frac{\partial \xi}{\partial t} + u \frac{\partial \xi}{\partial x} + u' \frac{\partial \xi}{\partial y} - \nu \left(\frac{\partial^2 \xi}{\partial x^2} + \frac{\partial^2 \xi}{\partial y^2} \right) - \frac{1}{\rho} \left(\frac{\partial F_y}{\partial x} - \frac{\partial F_x}{\partial y} \right) \right) d\Omega = 0 \quad (20)$$

The discretisation equation results in a series of discrete algebraic equations that take the form:

$$a_P \xi_P = \sum a_{nb} \xi_{nb} + b \quad (21)$$

where a_P terms are the active coefficients on ξ , and nb implies summation over the neighboring nodes (those to the West, W; East, E; South, S; and North, N) of P for two-dimensional computations, and b is the source terms.

The code generated is based on an unstructured mesh-generation. The nodes of the mesh for the coupling model electromagnetic-hydrodynamic are the same in the channel. At each time step, the electromagnetic and hydrodynamic problems can be solved alternatively and iteratively until convergence is reached.

We use the same steps for the thermal equation (19) as for the hydrodynamic equation (14):

$$\int_t^{t+\Delta t} \int_s \int_w \rho C_p \frac{\partial T}{\partial t} dx dy dt = \int_t^{t+\Delta t} \int_s \int_w \left[K \left[\frac{\partial^2 T}{\partial x^2} + \frac{\partial^2 T}{\partial y^2} \right] + \frac{J_i J_i^*}{2\sigma} \right] dx dy dt \tag{22}$$

with the source expression, the discretisation equation would still look like equation (21), but the coefficients would change. The new set is:

$$a'_p T_p = \sum a'_{nb} T_{nb} + b' \tag{23}$$

5. Simulations and Results

The potential vector \vec{A} is calculated for each finite element node by means of the finite element method. Hydrodynamic and thermal calculations supply, respectively, the velocity, the pressure components and the temperature which must be known at each integration point of the finite volume method.

For the coupling of the two methods F.E.M–F.V.M, it is necessary to ensure an adaptation of the grid mesh, i.e. we must find the same nodes for the two different methods. The electromagnetic force density calculated by the finite element method is introduced in the hydrodynamic equations which are solved using the finite volume method to determine the velocity and the pressure of the fluid in the channel. Also, the thermal source is calculated for the thermal problem.

Fig. 3 represents the coupling of the three problems (hydrodynamic-electromagnetic-thermal), and is divided into the following three parts:

- finite element method computation in the sinusoidal mode of the magnetic vector potential A by (2) and the computation of the force density by (5);
- finite volume method computation of the velocity in the transient state only in the channel of the MHD pump by using the vorticity vector–stream function equation (14). Once the stream function is determined, we can calculate the pressure at any point of the channel by the equation (16);
- finite volume method computation of the temperature in the transient state only in the channel of the MHD pump where the temperature is determined by the equation (19).

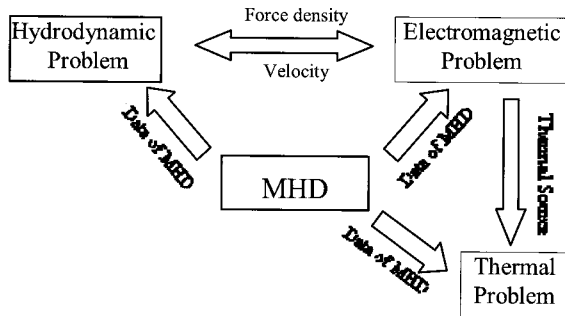


Fig. 3. The coupling scheme

For the electromagnetic problem the whole MHD pump is meshed, but for the hydrodynamic problem only the channel which contains the mercury liquid metal is meshed. The iterations are repeated until the error is low.

As results Figs. 4 and 5 represent respectively the magnetic induction and the distribution of the electromagnetic thrust in the MHD pump (this thrust is the same as that obtained by [3]).

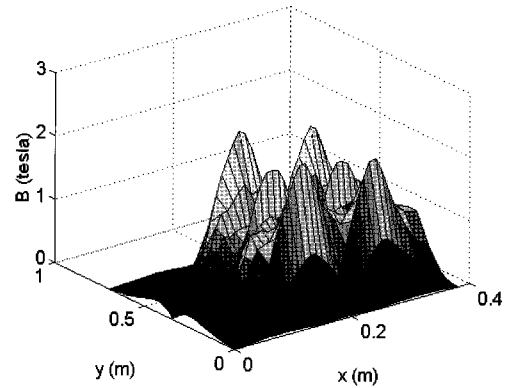


Fig. 4. The magnetic induction in the MHD pump

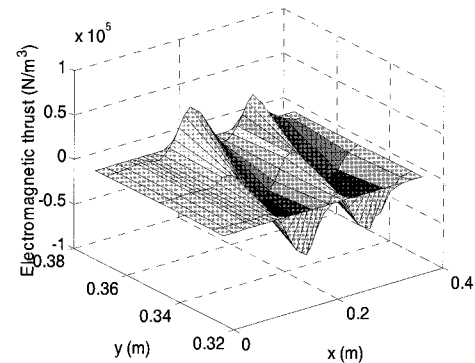


Fig. 5. The electromagnetic thrust

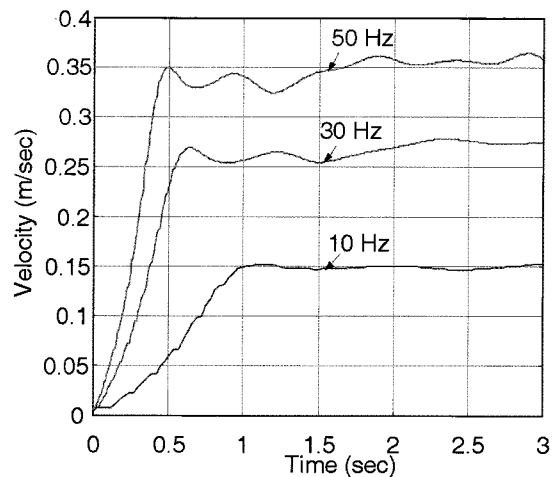


Fig. 6. Velocity in the middle of the channel for several frequencies

Fig. 6 represents the variation of the velocity of the pump for several frequencies. It is shown that the velocity increases as the frequency increases and a steady state is obtained after approximately two seconds.

Fig. 7 shows the pressure variations for several frequencies. It is found that the pressure increases as the frequency increases. It is important to notice that the amplitudes of the pressure oscillations increase with increasing frequency. Moreover, the “shock” values become more significant with a shorter transient state.

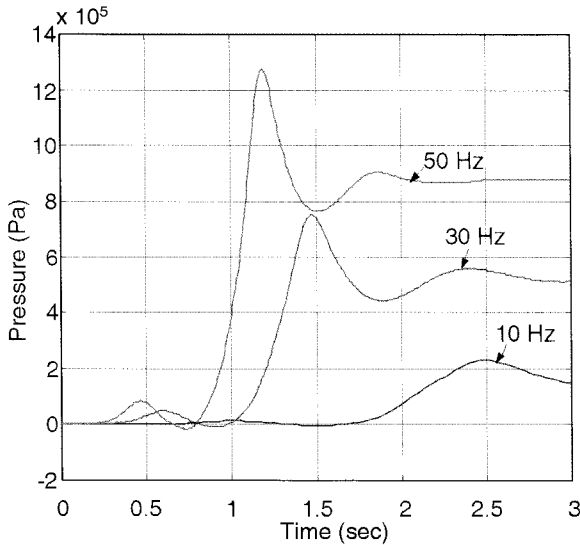


Fig. 7. Pressure in the middle of the channel for several frequencies

Fig. 8 shows the electric power density in the channel. The maximum induced power reaches $8 \cdot 10^6 \text{ W/m}^3$. The pace obtained is directly related to that of the eddy current density. This characteristic of the heat source is used in the numerical calculation of the temperature.

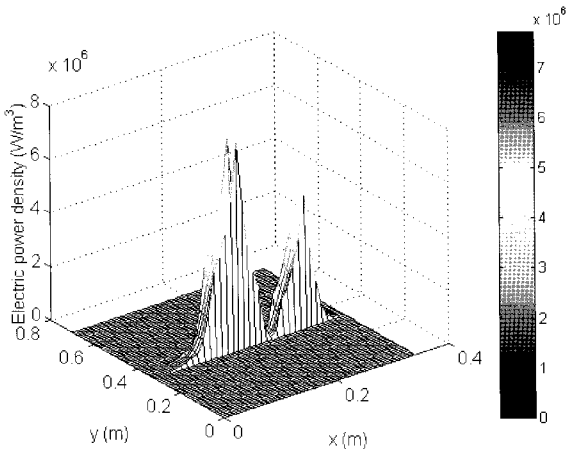


Fig. 8. The electric power density in the channel

Fig. 9 shows the distribution of the temperature for different frequencies. We denote the temperature increase

with the frequency. The maximum temperature for $f = 50 \text{ Hz}$ reaches $372 \text{ }^\circ\text{K}$.

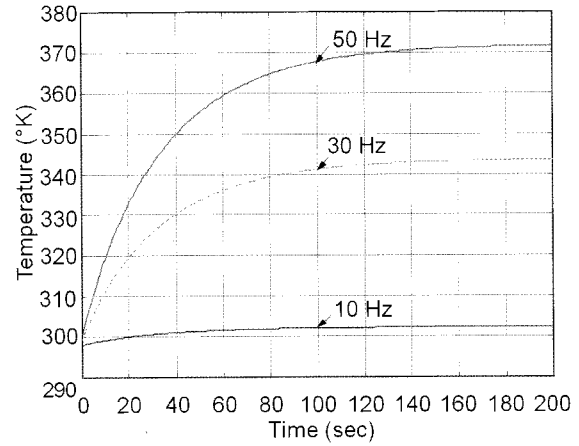


Fig. 9. Temperature in the channel for different frequencies

The following table gives the proprieties of the mercury:

Table 1. Parameters of the Mercury

Parameter	Value
Electrical conductivity (σ)	$1.0610^6 (\Omega \cdot \text{m})^{-1}$
Mass density (ρ)	$13.6 \cdot 10^3 (\text{kg} / \text{m}^3)$
Kinematic viscosity (ν)	$0.11 \cdot 10^{-6} \text{ m}^2 / \text{s}$
Specific heat (c_p)	$138 (\text{J} / \text{Kg } ^\circ\text{K})$
Thermal conductivity (K)	$8.4 (\text{W} / \text{m } ^\circ\text{K})$

6. Conclusion

The solution of the magnetohydrodynamic problem is obtained by using the \mathbf{A} , ξ , ψ and T formulations and the coupling of the 2D finite element-finite volume methods. We have disclosed the presence of fast transients and the oscillatory behavior in both velocity and pressure.

The obtained results confirm an influence of the frequency on the velocity and pressure distribution in the investigated flow [15] and [16].

A visualisation of the temperature curve leads to an appreciation of the effect of frequency on temperature in the channel. Furthermore, the obtained temperature results are identical to the results of [17].

References

[1] Berton, R., Magnetohydrodynamique, Editions Masson, 1991.
 [2] Vinsard, G., Laporte, B., and Takorabet, N., “An analysis of the rotationnel forces in the secondary of an electromagnetic pump”, *IEEE Transactions on Magnetics*, vol. 34, no .5, pp 3552-3555, Sept 1998.

- [3] Takorabet, N., "Computation of force density inside the channel of an electromagnetic pump by hermite projection", *IEEE Transactions on Magnetics*, vol. 42, no. 3, pp 430-433, March 2006.
- [4] Kadid, F. Z., Abdessemed, R., and Drid, S., "Characterisation of 2D Eddy Currents in the Channel of Linear Induction MHD Pump", *Journal of Electrical Engineering*, vol. 3, no. 2, pp 28-33, Romania, Dec 2003.
- [5] Kadid, F. Z., Abdessemed, R., and Drid, S., "2D FEM modeling of the linear induction MHD Pump taking into account the movement of the fluid", *AMSE Journals*, vol. 73, no. 4, pp 61-68, France, 2004.
- [6] Guermond, J. L., Mineev, P., and Shen, Jie, "An overview of projection methods for incompressible flows", *Computer methods in applied mechanics and engineering*, ELSEVIER, pp 6011-6045, 195, 2006.
- [7] Verardi, S.L.L., Cardoso, J.R., and Costa, M.C., "Three dimensional finite element analysis of MHD duct flow by the penalty function formulation", *IEEE Transactions on Magnetics*, vol. 37, no. 5, pp.3384-3387, Sept 2001.
- [8] Patankar, S. V., *Numerical Heat Transfer Fluid Flow*, Hemisphere Publishing Corporation, 1980.
- [9] Anderson, D. A., Tannehill, J. C., and Pletcher, R. H., *Computational Fluid Mechanics and Heat Transfer*, Hemisphere Publishing Corporation, 1984.
- [10] Krzeminski, S. K., Smialek, M., and Wlodarczyk, M., "Numerical Analysis of Peristaltic MHD flows", *IEEE Transactions on Magnetics*, vol. 36, no. 4, pp 1319-1324, July 2000.
- [11] Nesliturk, A. I., and Tezer-Sezgin, M., "Finite element method of electrically driven magnetohydrodynamic flow", *Journal of Computational and Applied Mathematics*, ELSEVIER, pp 339-352, 192, 2006.
- [12] Tezer-Sezgin, M., Aydin, S. Han, "Solution of magnetohydrodynamic flow problems using the boundary element method", *Engineering Analysis with Boundary Elements*, ELSEVIER, pp 411-418, 30, 2006.
- [13] Sadiku, M. N. O., *Numerical Techniques in Electromagnetics*, CRC Press, 1992.
- [14] Jin, Jianming, *The Finite Element Method in Electromagnetics*, John Wiley & Sons, 1993.
- [15] Yamagushi, T., Kawase, Y., Yoshida, M., Saito, Y., and Ohdachi, Y., "3-D finite element analysis of a linear induction motor", *IEEE Transactions On Magnetics*, vol. 37, no. 5, pp 3668-3671, Sept 2001.
- [16] Affanni, A., and Chiorboli, G., "Numerical modeling and experimental study of an AC magnetohydrodynamic (MHD) pump", *IMTC-Instrumentation and Measurement Technologie Conference*, Sorrento, Italy, IEEE, pp 2249-2253, 24-27 April 2006.
- [17] Ghassemi, M., and Pasandeh, R., "Thermal and Electromagnetic analysis of an Electromagnetic launcher," *IEEE Transactions On Magnetics*, vol. 39, no. 3, pp 1819-1822, May 2003.

Dr. Fatima Zohra KADID was born in Batna, Algeria, in 1968. She received her B.Sc., M.Sc. and Ph.D. degrees from Electrical Engineering Institute of Batna University, Algeria, in 1991, 1995 and 2004, respectively. Currently, she is an Associate Professor at the Electrical Engineering Institute, University of Batna, Algeria. She is also a member of the LEB Research Laboratory. Her research interests are the design of electrical machines, magnetic bearings and renewable energy.



Saïd DRID was born in Batna, Algeria, in 1969. He received his B.Sc., M.Sc. and Ph.D. degrees in Electrical Engineering from the University of Batna, Algeria, in 1994, 2000, and 2005, respectively. Currently, he is an Associate Professor at the Electrical Engineering Institute, University of Batna, Algeria. He is the head of the "Energy Saving and Renewable Energy" team in the Research Laboratory of the Electromagnetic Induction and Propulsion Systems of Batna University. His research interests include electric machines and drives, renewable energy, field theory and computational electromagnetism. He is also a reviewer for IET Theory Control & Applications journal, IET Renewable Power Generation journal, PCN Journal of Physical and Chemical News, JAFM Journal of Applied Fluid Mechanics, and IJSS International Journal of Systems Science.



Pr. Rachid Abdessemed was born in Batna, Algeria, in 1951. He received his M.Sc. and Ph.D. degrees in Electrical Engineering from Kiev Polytechnic Institute, Kiev, Ukraine, in 1978 and 1982, respectively. He has been working for more than 28 years with the Department of Electrical Engineering, University of Batna, as a Professor. Currently, he is Director of the Electrical Engineering Laboratory. His current area of research includes design and control of induction machines, reliability, magnetic bearing, and renewable energy.